Biomedical Signal Processing and Control xxx (2010) xxx–xxx

Contents lists available at ScienceDirect

Biomedical Signal Processing and Control

journal homepage: www.elsevier.com/locate/bspc

Tremor analysis by decomposition of acceleration into gravity and inertial acceleration using inertial measurement unit

Otakar Šprdlík[a,b], Zdeněk Hurák[b,*], Martina Hoskovcová[c], Olga Ulmanová[c], Evžen Růžička[c]

[a] Institute of Information Theory and Automation of the ASCR, Pod Vodarenskou vezi 4, CZ-182 08, Prague 8, Czech Republic
[b] Czech Technical University in Prague, Faculty of Electrical Engineering, Dept. of Control Eng, Technická 2 16627, Praha 6, Czech Republic
[c] Charles University in Prague, First Faculty of Medicine, Dept. of Neurology and Centre of Clinical Neuroscience, Czech Republic

ARTICLE INFO

Article history:
Received 4 January 2010
Received in revised form 25 August 2010
Accepted 16 September 2010
Available online xxx

Keywords:
Tremor
Accelerometer
Inertial measurement unit
Gravitational artifact
Regression
Tremor rating scale

ABSTRACT

Decomposition of acceleration was investigated as an alternative to commonly used direct spectral analysis of measured acceleration or angular velocity for tremor quantification. An orientation estimation algorithm was devised to decompose the measured acceleration into the gravitational artifact and the inertial acceleration caused by sensor movement in an inertial reference frame. Resulting signals, beside the measured acceleration and angular velocity, were used to assess tremor amplitude and frequency by spectral peak detection. The algorithm was tested on experimental data from a clinical study including patients with essential tremor. The testing comprised of the classification of measurements to come from a patient or a healthy control and of the regression of the visual assessment of tremor amplitude. Small improvements in performance measures were achieved by using the decomposed acceleration. The regression accuracy was comparable to the accuracy achieved in other works. The influence of sensor calibration and connections of results to an analytic approach were analyzed briefly.

1. Introduction

Tremor is defined as a rhythmical, involuntary oscillatory movement of a body part [1]. Its quantification is necessary for clinical monitoring as well as for studies of movement disorders featuring tremor [2]. Clinical examination with various rating scales has been the most frequently used approach, although inertial sensors have also become widely used in research studies. Direct spectral analysis of signals measured by accelerometers has mostly been employed. This, however, may lead to several problems including the contamination of the measured linear acceleration by the variable projection of gravity, which implies the deterioration of a simple estimate of displacement (or its amplitude) using double integrated acceleration, as used for instance in [2,3]. A component of the gravitational artifact may have a frequency that is double of the frequency of tremor due to the non-linear properties of the periodic alternate movement with a rotational character [4]. However, such frequency doubling may be present even in the movement acceleration.

These problems can be reduced by a suitable arrangement of the test procedure and a choice of the most suitable sensor axis for the analysis. In a typical case the measurement is conducted with the patient's hands kept horizontally and only the sensor axis that is approximately vertical is processed [2,5,6]. In addition, the hand motion can be restricted as in [3]. This case is analyzed with the use of a simplified model of a hand in [4]. Nevertheless, analysis of just one sensor axis obscures the other movement components and the choice of the vertical axis is not always appropriate, especially if some movement task is to be accomplished, like in tests for intention tremor.

A different approach to cope with the gravitational artifact may be the use of the magnitude of the 3D output of a triaxial accelerometer. The main idea is that the magnitude is steady and equals gravity if no linear acceleration is applied to the sensor, even if the sensor changes its orientation in time [7,8]. Besides sacrificing the possibility to estimate the direction of the movement when using only the magnitude of the signal, the measured magnitude minus gravity does not exactly correspond to the amplitude of the acceleration caused by linear movement because it depends also on the direction of the movement with respect to gravity. Moreover, a movement with rotational character may produce some additional DC component in the magnitude while the alternating component may be quite low. Therefore, the amplitude of such a tremulous movement may be underestimated when using the AC component of the magnitude. Nevertheless, the magnitude-based approach

* Corresponding author. Tel.: +420 224357682; fax: +420 286890286.
E-mail addresses: sprdlik@utia.cas.cz, sprdlo1@fel.cvut.cz (O. Šprdlík), hurak@fel.cvut.cz (Z. Hurák), mhosk@lf1.cuni.cz (M. Hoskovcová), ovesel@lf1.cuni.cz (O. Ulmanová), eruzi@lf1.cuni.cz (E. Růžička).

1746-8094/$ – see front matter © 2010 Elsevier Ltd. All rights reserved.
doi:10.1016/j.bspc.2010.09.004

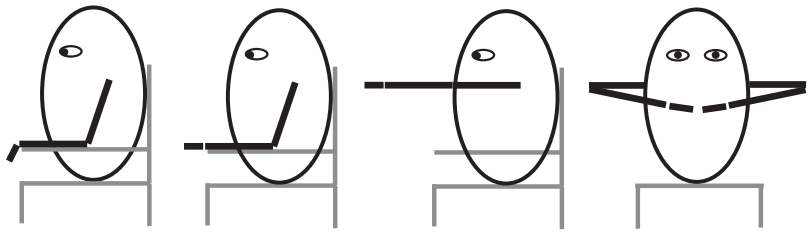

Fig. 1. Sketch of tasks conducted to test rest and postural tremor.

was used in several studies to roughly quantify a movement [9] of tremor [10].

Alternative sensors have also their own disadvantages: MEMS gyroscopes [11–14] may be a good choice especially for the cases where the movement is limited to a particular joint near to the site of measurement, or if sensors are placed at several segments of the arm [12], but they also obscure some more complex movements. Displacement sensors like mechanical devices [15], camera kinematic systems [16], and magnetic systems [17] are usually bulky and expensive. Moreover, the limited resolution of common camera systems makes the analysis of a very mild tremor infeasible.

Attitude estimation using measured data from both accelerometers and gyroscopes is a way to decompose the measured acceleration into the gravitational and motional components, hence it makes short-time estimates of displacement by double integration feasible. The bulky size of an inertial measurement unit (IMU) used to be the limiting factor, but with the advances in MEMS based devices, this is no longer a major issue. Nowadays, even devices containing accelerometers and gyroscopes suitable for fixing to a human finger are available – Kinesia™ by CleveMed [14]. However, in the present work, slightly larger units were used.

The task of tremor measurement by a set of inertial sensors that allow decoupling from the gravitational artifact was already dealt with in several works: [18] proposed a pure-accelerometer system for tremor sensing and active compensation of surgeon's tremor in a microsurgical instrument with accelerometer units fixed 10 cm apart from each other. The size of one of the units was reduced in [19], but the need of the two distant sites on a rigid body remains. In [20] a system was designed for estimation of an upper limb orientation from inertial sensors placed at several sites on the arm. Sensitivity analysis with the use of simulations demonstrated its proficiency at frequencies of tremor. The proficiency was also demonstrated by means of comparison with the measurement by a mechanical device. The angle of an elbow joint manifesting tremor was the observed quantity. However, in this approach a mathematical model of the arm and a set of several sensor units are needed. In [14] gravity was not explicitly decoupled from accelerometer measurement, although sensors potentially allowed it. Rather, clinical scores were regressed by linear models with several features of the measured signals acting as inputs.

The goal of our study was to demonstrate the feasibility of quantifying tremor using the decomposition of the signal registered with accelerometers into the gravitational and movement components by inertial estimation of orientation (attitude). This is to make the tremor quantification as independent as possible from the orientation and the direction of movement of the observed body segment relative to gravity. Frequency spectrum-based features of the measured signals and of the outputs of the decomposition were extracted and their performance was compared in two tasks,

- to classify a single measurement from one hand or both hands to come from a patient or a healthy control, provided only the information that the measurement is from a test for postural hand tremor, without the knowledge of the particular task,
- to predict a visual assessment of tremor amplitude by clinicians, without the knowledge of the type of tremor (rest/postural) and particular task. The performance of the regression was compared to results of other works.

A regression of a visual tremor assessment by quantities from an instrumented assessment was already done in a number of studies. Part of them deal with long-term ambulatory monitoring of tremor (e.g. [13,21–23]), other with short measurements in defined hand positions (e.g. [14,15,24,25]).

2. Methods

2.1. Subjects

The algorithm was used to quantify tremor on a sample of 59 subjects: 30 patients with essential tremor diagnosed according to the clinical criteria [1], age (mean ± standard deviation) 55.8 ± 18.1 years (range 19–81), disease duration 24.8 ± 16.5, Fahn-Tolosa-Marín Tremor Rating Scale score [26] 27.0 ± 13.4 (range 9–67), 8 females, and 29 healthy individuals without any tremor-inducing disorder, age 53.8 ± 17.4 years (range 19–81), 8 females.

2.2. Experimental setup and data acquisition

Hand tremor was measured in several conditions, all with the subjects sitting in an armchair (see Fig. 1),

- forearms leaned on the armrests and hands hanging freely down,
- forearms leaned on the armrests and hands extended forward horizontally,
- arms held forward horizontally towards a horizontal target placed in front of the subject at the height of shoulders, hands pronated,
- "wing" position.

The first task is intended for the assessment of the *rest tremor*. The other tasks are intended for the assessment of the *postural tremor*. Tests lasted 20 s and were conducted twice (except for two subjects). Totally, 464 recordings of tasks to test the rest and postural tremor were acquired with sensors placed on both hands, that means 928 recordings from a hand in a test were obtained. Whole trials were 8–15 min long and included also tests for the intention tremor.

Integrated inertial measurement units MTx® by Xsens® were placed on subjects' hand dorsa over third and fourth metacarpal bones using neoprene bands with hook-and-loop fasteners. The units measure acceleration, angular rate, and local magnetic field in three axes. Internally computed estimates of the orientation may be acquired too. The measured quantities were transmitted with the sampling frequency of 100 Hz by cables to a personal computer and acquired using our own software. The software served also to identify starts of the tests by pressing keys on the PC keyboard by one of investigators. The internal orientation estimates provided

Please cite this article in press as: O. Šprdlík, et al., Tremor analysis by decomposition of acceleration into gravity and inertial acceleration using inertial measurement unit, Biomed. Signal Process. Control (2010), doi:10.1016/j.bspc.2010.09.004

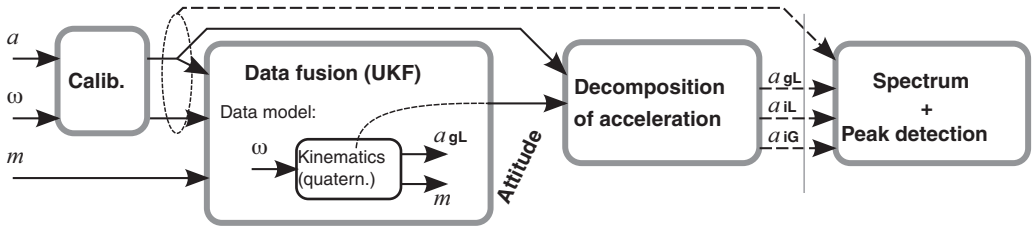

Fig. 2. Block scheme of estimation and quantification.

by the unit were not acquired because in our original clinical study we were only interested in the acceleration. Moreover, technical problems with the software at the beginning of the study hindered the acquisition of orientation estimates.

2.3. Preprocessing and inertial estimation

Time-varying gyroscope biases may produce large errors in the estimation of orientation. To reduce them, they were calibrated out in each measurement trial using the following scheme. The intensity of movement was quantified by means of variation of the gyroscope signal ω and the filtered accelerometer signal a (low-pass, 8 Hz) in 0.3 s segments. Segments with RMS of standard deviations over the 3 axes (σ_a, σ_ω) lying below the predefined threshold (0.1 m s^{-2} and 0.05 rad s^{-1} for accelerometer and gyroscope, respectively) were marked as quasistatic. Each segment was characterized by its mean measured angular rate, σ_a, and σ_ω. Consecutive segments with similar properties were joined. Gyroscope bias was then estimated as the mean angular rate in the quasistatic segments. Similar approach was used for the calibration of accelerometers in several calibration sessions. The sensor was rotated into 6 different inclinations and the measurements were segmented as described above. The biases and gains of the accelerometers were obtained using the quasistatic state approach [27] with the use of a different optimization procedure [28] and $1/\sigma_a^2$ as weights in the optimization criterion.

The orientation estimate provided by IMU was not acquired in real-time during measurement, instead, we applied own estimation of orientation with the use of calibrated data off-line. The unscented Kalman filter (UKF) [29,30] was used to fuse the information from IMU data (linear acceleration in 3 axes, angular rate around 3 axes and 3 components of local Earth magnetic field). The UKF was chosen as the tool because the unscented transform can propagate covariances better through a nonlinear system than the more commonly used Extended Kalman filter (EKF) using linearization of the system equations. Better accuracy of UKF compared to EKF was demonstrated in a navigation application involving a nonlinear equation of quaternion update [31]. Quaternion update is a fundamental part of our model too. The filter forms the UKF block in Fig. 2.

First three blocks represent preprocessing and inertial estimation, the last block represents amplitude and frequency extraction. Values a, ω, m are the acceleration, angular rate and local magnetic field, respectively, measured in the coordinate system of the measurement unit. Decomposition outputs are a_{gL} (gravitational artifact), a_{iL} (acceleration due to movement observed in the sensor frame), and a_{iG} (the same quantity transformed into the inertial frame).

The data fusion filter is based on quaternion representation of kinematics. Quaternions and their algebra provide an efficient tool for representing rotations in 3D lacking the gimbal lock of 3-angle systems (e.g. Euler angles) and using only four numbers ($q = [q_0\, q_1\, q_2\, q_3]^{\mathrm{T}}$) instead of nine in 3×3 rotation matrices, see for example [32]. The rotation from an Earth-fixed inertial reference frame to the reference frame of the sensor was used to represent the orientation of the sensor. The rotation matrix R corresponding to a known quaternion with unit size may be expressed for example by

$$R = \begin{bmatrix} q_0^2 + q_1^2 - q_2^2 - q_3^2 & 2(q_1q_2 + q_0q_3) & 2(q_1q_3 - q_0q_2) \\ 2(q_1q_2 - q_0q_3) & q_0^2 - q_1^2 + q_2^2 - q_3^2 & 2(q_2q_3 + q_0q_1) \\ 2(q_1q_3 + q_0q_2) & 2(q_2q_3 - q_0q_1) & q_0^2 - q_1^2 - q_2^2 + q_3^2 \end{bmatrix}. \quad (1)$$

The quaternion representation of the orientation forms the state vector of the data fusion filter. The angular velocity acts as an input. The projection of gravity and the projection of the local Earth magnetic field to the sensor coordinate frame are model outputs. The continuous quaternion update equation and output equations are

$$\dot{q}(t) = \frac{1}{2}[\Omega(t)]q(t), \quad (2)$$

$$a_{gL}(t), = R(q(t))[0\ 0\ g]^T, \quad (3)$$

$$m(t) = R(q(t))m_0,\ m_0 = [\cos(\phi_m)0 - \sin(\phi_m)]^{\mathrm{T}}, \quad (4)$$

where q is the quaternion of the rotation from the global reference frame to the local frame of sensor, $R(q)$ is the corresponding rotation matrix, a_{gL} is the projection of gravity to the local reference frame, g is the size of gravitational acceleration, m is the estimated direction of the magnetic measurement, φ_m is the local magnetic inclination, and $[\Omega]$ is the matrix defined by the angular rate ω as follows, (time argument omitted)

$$[\Omega] = \begin{bmatrix} 0 & -\omega_x & -\omega_y & -\omega_z \\ \omega_x & 0 & \omega_z & -\omega_y \\ \omega_y & -\omega_z & 0 & \omega_x \\ \omega_z & \omega_y & -\omega_x & 0 \end{bmatrix}. \quad (5)$$

Approximate Euler discretization of the quaternion update was used as the state update equation in the model,

$$q(t_{k+1}) = f(q(t_k), \omega(t_k)) = q(t_k) + \frac{1}{2}[\Omega(t_k)]q(t_k)T_s, \quad (6)$$

where T_s denotes the sampling period (0.01 s in our case). To ensure numerical stability of the quaternion estimate, it was divided by its amplitude between samples. Hence, the norm of the quaternion was forced to equal one. The (calibrated) measured angular rate ω was used as the input. The output measurements were

- measured acceleration a as a measure of the projection of gravity (that is a good measure under static conditions),
- measured vector of magnetic field – the sensors used were calibrated to give vectors of amplitude approximately 1 in non-corrupted Earth magnetic field.

In a standard setting, Kalman filter assumes exactly known inputs. That is not our case because of the noisy measurement of the angular velocity. The noise was taken into account using a covariance added to the process noise covariance in the model as shown for linear systems in [33]. The instant linearization of discretized quaternion update equation (6) at the estimated quaternion was

Please cite this article in press as: O. Šprdlík, et al., Tremor analysis by decomposition of acceleration into gravity and inertial acceleration using inertial measurement unit, Biomed. Signal Process. Control (2010), doi:10.1016/j.bspc.2010.09.004

used as the input matrix, (time argument omitted)

$$B = \frac{\partial f(q,\omega)}{\partial \omega} = \frac{1}{2} T_s \begin{bmatrix} -q_1 & -q_2 & -q_3 \\ q_0 & -q_3 & q_2 \\ q_3 & q_0 & -q_1 \\ -q_2 & q_1 & q_0 \end{bmatrix}. \quad (7)$$

Then the process noise covariance used was

$$Q(t_k) = B(t_k) V_\omega B^T(t_k) + \varepsilon_p I_4, \quad (8)$$

where V_ω is the covariance of the gyroscope measurement noise, ε_p is a small constant (10^{-12} was used), and I_4 is diagonal matrix. The small diagonal term was used as imaginary process noise to cope with errors caused by the discretization and to ensure positive definiteness of Q.

Simple rules modifying the observation covariance matrix were incorporated to reduce influence of magnetic disturbances and influence of movement to the accelerometer as a sensor of gravity. The rules are based on differences between the magnitudes of the measured acceleration and magnetic field vectors and the expected sizes.

$$R_a(t_k) = V_a + k_a N_a^2(t_k) I_3;\ R_m(t_k) = V_m + k_m N_m^2(t_k) I_3, \quad (9)$$

where V_a and V_m are covariances of accelerometer and magnetometer noise, respectively. Local relative discrepancies between found and expected amplitudes of measured signals as measures of the model outputs are defined

$$N_a(t_k) = WA\left(\frac{|||a(\tau)||_2 - g|}{g}\right);\ t_k - n \le \tau \le t_k + n, \quad (10)$$

$$N_m(t_k) = WA(|||m(\tau)||_2 - 1|);\ t_k - n \le \tau \le t_k + n, \quad (11)$$

where operation WA stands for a weighted average. The averaging is a filtering by a noncausal FIR filter with length $2n+1$. The length used was 3 ($n=1$) and weights [0.25 0.5 0.25]. Constants $k_a = 200$ and $k_m = 2$ were found experimentally by iterating on their values and comparing a known displacement with the displacement estimated by double numerical integration of the movement acceleration estimated via the orientation estimation procedure – sensor was moved several times by hand from one place and put back or to another place at known distance.

The Unscented Kalman filter was implemented using ReBEL Toolkit [34] in Matlab® without particular focus on computational efficiency. Having obtained the estimates of orientation, gravity was projected to the sensor reference frame and subtracted from the measured acceleration. Finally, we analyzed five 3D signals,

- a measured acceleration, calibrated,
- a_{gL} estimated projection of gravity to the local frame, called also gravitational artifact or component in the text, $a_{gL}(t_k) = R(t_k) \cdot [0\,0\,g]^T$, where $R(t_k)$ is the rotation matrix determined by the estimated quaternion,
- a_{iL} estimated acceleration due to movement in an inertial reference frame, observed in the local (sensor) frame, called also inertial acceleration or component in the text, $a_{iL}(t_k) = a(t_k) - a_{gL}(t_k)$,
- a_{iG} inertial acceleration observed in the global inertial reference frame, $a_{iG}(t_k) = R^T(t_k)\, a_{iL}(t_k)$,
- ω measured angular velocity, with estimated bias removed.

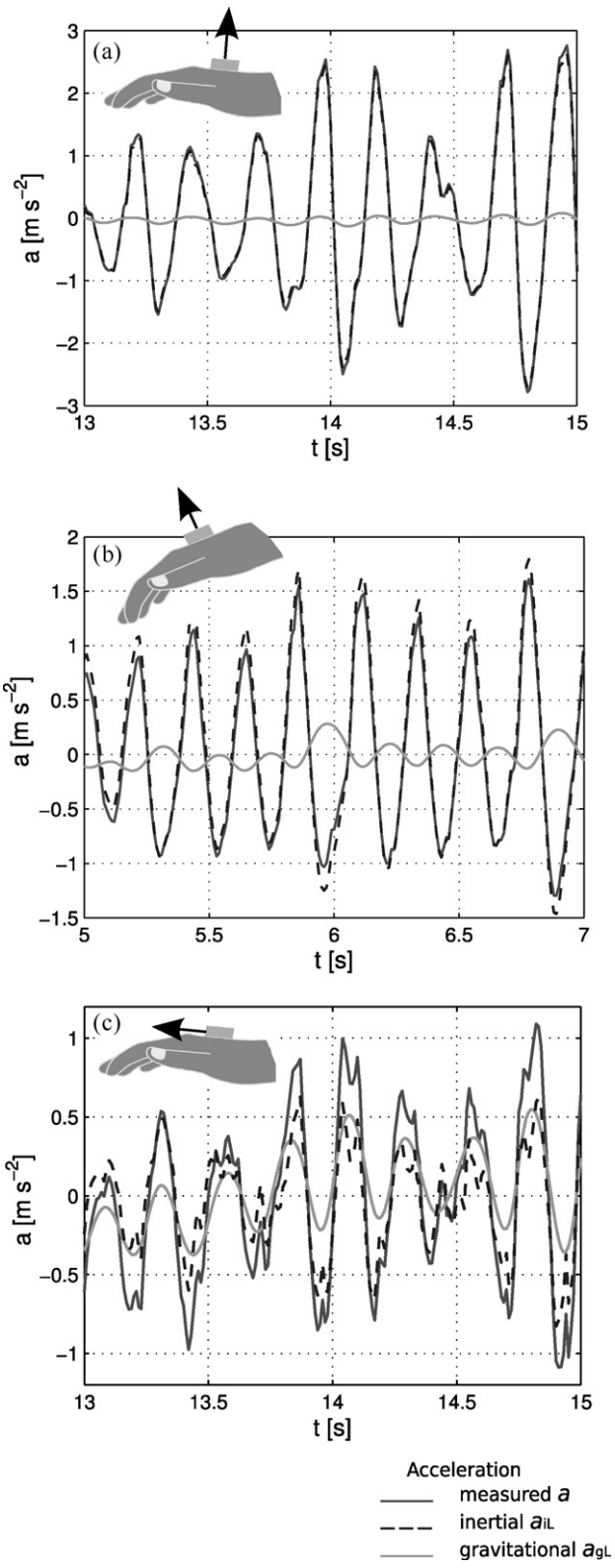

Fig. 3. Examples of decomposition.

See Fig. 3 for examples of the acceleration decomposition. The obtained inertial acceleration can be transformed to the global reference frame and potentially used for an estimation of position by double integration (Fig. 4).

The signals were measured with the same patient: (a) and (c) are from the first test on postural tremor, (b) is from the test on rest tremor. Approximate hand positions and the used axes are displayed. Means were subtracted from a and a_{gL} signals to get plots ranging around zero.

The displacement estimate (mm) in a one-second interval of a measurement of relatively strong tremor is displayed (gray). The double integration of a_{iG} was combined with high pass filtering

Please cite this article in press as: O. Šprdlík, et al., Tremor analysis by decomposition of acceleration into gravity and inertial acceleration using inertial measurement unit, Biomed. Signal Process. Control (2010), doi:10.1016/j.bspc.2010.09.004

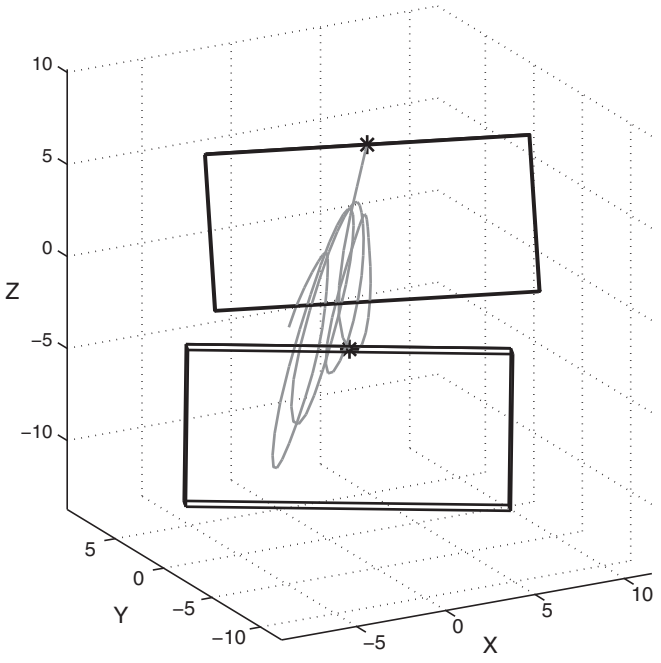

Fig. 4. Example of tremor movement reconstructed by inertial estimation.

to eliminate drift caused by the integration of errors in a_{iG}. The estimated orientation of the sensor is visualized at two instants (stars), 0.1 s apart, using black line boxes (16 mm × 12 mm × 8 mm).

Sensors are subject to errors, especially biases that deteriorate the quality of orientation estimate and consequently our tremor detection scheme. We did some calibration as noted above. But even if the initial calibration had been perfect, errors could arise from the drift of biases. Therefore, check was made for additional errors in measured quantities. Namely, biases of $0.02\,\mathrm{m\,s^{-2}}$ and $0.01\,\mathrm{rad\,s^{-1}}$ were added to Y axes of accelerometers and gyroscopes, respectively. The errors are approximately of the size of the biases found in single axes of the sensors used: Biases of the two accelerometers found in one of the calibration sessions were $[-0.019\ 0.027\ -0.017]$ and $[0.021\ -0.054\ -0.043]\,\mathrm{m\,s^{-2}}$. Gyroscope biases found in the 59 measurement sessions were (mean ± standard deviation) $[0.001 \pm 0.004,\ 0.004 \pm 0.002,\ 0.017 \pm 0.002]\,\mathrm{rad\,s^{-1}}$ for one gyro and $[-0.030 \pm 0.005,\ 0.015 \pm 0.002,\ 0.022 \pm 0.003]\,\mathrm{rad\,s^{-1}}$ for the second one.

The acceleration was decomposed twice in addition to the original decomposition – using a corrupted by the constant bias and using ω corrupted by the constant bias. The resulting acceleration components were fed to the peak quantification scheme. Obtained amplitudes were compared to the amplitudes of the components derived using the original, calibrated, measurements.

2.4. Amplitude and frequency extraction

Fast Fourier transform was used to quantify tremor frequency and amplitude as it is widely used technique in the field [2,3,5,6,11,14,15] and provides a straightforward representation of frequency distribution of the signal amplitude. As alternatives, time-domain algorithms based on thresholds [21], parametric identification methods [13,35], and techniques based on empirical mode decomposition (EMD) [12] have been proposed in the literature.

First, means were removed from signals. Then, power spectral density (PSD) was computed for every component of a 3D signal via a filtered periodogram. The periodogram was smoothed by a weighted moving average with the window of width approximately 1 Hz and triangular weights b defined by

$$b(k) = \frac{hl - |k|}{\sum_{m=-hl+1}^{m=hl-1} hl - |m|};\ -hl < k < hl;\ hl = round\left(\frac{0.5}{\Delta f}\right);\ \Delta f = \frac{F_s}{dl}, \quad (12)$$

where F_s is the sampling frequency (Hz), Δf frequency step in the periodogram (Hz), dl data length (samples), hl length of a half of the averaging window (number of frequency steps), and b is the vector of filter coefficients.

This method gives a high frequency resolution compared to averaged periodogram. The length was chosen based on the heuristic idea not to oversmooth the periodogram and on our visual observations (see Fig. 5 for examples). The length of 1 Hz coincides with the choice in [36], where it was used to get an initial estimate of PSD to start a more complex adaptive scheme.

Frequency distribution of power of 3D signal was computed as a sum of the three PSD. Peaks were detected in the composite PSD by the following algorithm.

1. in the interval 1–15 Hz find all local minima and maxima between them,
2. reduce the number of maxima to get the set of highest maxima separated from each other by minima deep at least 3 dB (with the value half the lower of the resting neighbor maxima),
3. take the position of the highest resting maximum between 3.5 and 12 Hz as tremor frequency f_α, where α stands for the name of the signal used (a, a_{iL}, a_{iG}, a_{gL}, or ω).

Usually, this algorithm gives the same frequency as a simple position of the maximum of PSD in the interval 3.5–12 Hz. The difference was especially in the cases where a non-tremor movement produces a low frequency artifact with amplitude higher than the tremor peak and with falling slope of PSD crossing the lower boundary of the frequency range of tremor (Fig. 5, in the middle), and in the cases where there was no marked peak (no peak separated from the rest of PSD by sufficiently deep minima). The first situation may arise especially in measurements where a combination of marked voluntary movement and tremor occurs. An alternative to cope the voluntary movement could be found with the use of parametric methods or EMD [12,37].

For each signal α (α standing for a, a_{iL}, a_{iG}, a_{gL}, or ω), its amplitude A_α, called also tremor amplitude in the text, was determined. The amplitude (effective value) was computed as the square root of the numerical integral of PSD in the ±1 Hz neighborhood of the detected frequency f_α. The width of 2 Hz was found enough to cover the width of typical peaks, although in some cases parts of sidelobes were missing (Fig. 5). When no peak was detected, the amplitude was set to zero.

Composite PSD estimates of 3D accelerometer signals from three measurements. Thin line corresponds to the periodogram method; thick line corresponds to the method of filtered periodogram. Dashed line corresponds to the PSD estimate of the inertial component of acceleration. Two vertical lines mark ±1 Hz neighborhood of the peak frequency.

2.5. Correlations of amplitudes and frequencies detected for different signals

The signals (a, a_{iL}, a_{iG}, a_{gL}, ω) were compared in terms of Pearson's linear correlation coefficients between the amplitudes (A) and between the frequencies (f) derived from the peaks detected in their spectra. The cases where no peaks were detected in some of the signals were removed from this analysis.

Please cite this article in press as: O. Šprdlík, et al., Tremor analysis by decomposition of acceleration into gravity and inertial acceleration using inertial measurement unit, Biomed. Signal Process. Control (2010), doi:10.1016/j.bspc.2010.09.004

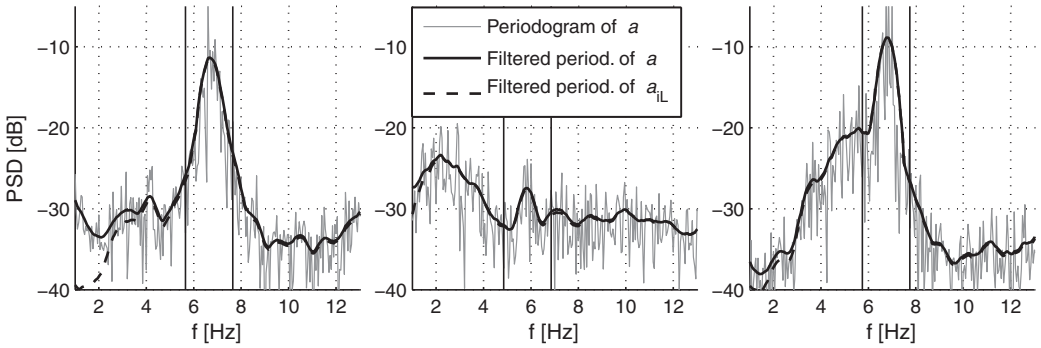

Fig. 5. Examples of PSD estimate.

Amplitudes may range over several decades, and then linear correlation coefficients between raw amplitudes may be dominantly determined by several highest amplitudes. Logarithms of amplitudes reduce the influence of highest values to correlation coefficients. They were also found to be linearly related to tremor severity as rated by clinicians [24]. Therefore, correlations of amplitude logarithms were computed too.

2.6. Alignment with hand axes

Part of the measurements was also treated in more detail via the calculation of amplitudes in individual axes. Estimated axes of hands were used instead of axes of sensors. The relative orientation of hand and sensor axes was determined from the task with arms held forward towards a horizontal target. Rotation matrices were computed using following rules. Axes Z of hands are considered to be vertically heading up during the test. Axes X are considered to be parallel to the average of projections of sensor's axes X (aligned approximately to proximodistal axes of hands) to horizontal plane. Axes Y then head horizontally to the left from the view of the subject. Amplitudes obtained for the inertial and gravitational components in the estimated axes were compared.

2.7. Differences between groups

The group of patients with essential tremor and the group of healthy subjects were compared in averages and variances of amplitude logarithms. The amplitude of the acceleration a_Z measured in the direction perpendicular to the hand was analyzed beside the amplitudes of the 3D signals.

In cases where no peak was detected the amplitude was set to a small value to get a finite logarithm. The value chosen was 0.0025 for A_{aZ}, 0.01 for A_a, A_{aiL}, and A_{aiG}, 0.001 for A_{agL} and 0.005 for A_ω, that is near to the least nonzero amplitude (0.0025, 0.0114, 0.0107, 0.0012, 0.0052 for $A_{aZ}, A_a, A_{aiL}, A_{agL}, A_\omega$, respectively). Such a limited logarithm of an amplitude A_α is denoted L_α.

Two-sample t-test was accomplished to trace differences between the groups. It was applied to amplitude logarithms from

- the test for rest tremor,
- all the tests for postural tremor taken together.

Two parameters of *receiver operating characteristic* (ROC) curves were extracted for the amplitudes from all the tests for postural tremor taken together,

- the area under the ROC curve (AUC),
- potential percentage of correct classification of the signal to come from the group of patients or controls based on its amplitude.

First, all the parameters were obtained for the scenario that the amplitude derived from the signal only in one hand in one test was used to classify the subject as a patient or as a control. In the second scenario, the greater of the amplitudes from the left and right hand in one test was used. Note that in the first scenario the number of samples was twice the number of samples in the second scenario because the amplitudes from the left hand and from the right hand were taken separately.

2.8. Regression of visual assessment

In part of the measurements (177 tests with 21 patients and two controls), a video of hands and arms of subjects was recorded simultaneously with the acquisition of inertial data. Tremor amplitude in both hands was assessed from the video recordings by two trained clinicians according to the amplitude assessment in the Fahn-Tolosa-Marín Tremor Rating Scale (0, 1, 2, 3, 4). When scores assessed by the two clinicians differed, the average was used for statistical analysis. Totally, 354 scores of a hand tremor were obtained (177 tests, 2 hands).

The score was regressed using the linear least squares method. The regression functions were polynomials with the logarithms (limited, see the previous section) of the obtained amplitudes as variables. Polynomials in a single amplitude logarithm were used with the degree up to 15. 2D polynomials were used with total degree up to 15. 3D polynomials were used with total degree up to 13. For example, the total degree of 2D polynomial in L_a, and L_ω, $b_{00} + b_{10}\ L_a + b_{01}\ L_\omega + b_{11}\ L_a\ L_\omega + b_{02}\ L_\omega^2 + b_{12} L_a L_\omega^2$, is considered to be 3 (1 in L_a and 2 in L_ω).

The *leave-one-out* method was used to verify the ability of the different polynomial structures of the regression function to predict the visual assessment. One visual score and the corresponding set of amplitudes were left out each time. The *root mean squares error* (RMSE), *mean absolute error* (MAE), *coefficient of determination* (r^2), and percentage of predictions with error lower than 1 ($\%_{E<1}$) were computed as the measures of regression accuracy.

3. Results

3.1. Influence of sensor biases

The amplitudes of acceleration components obtained using the acceleration measurement corrupted by the additional bias and using the angular rate measurement corrupted by the additional bias were compared to the amplitudes of acceleration components obtained using the calibrated data, see Table 1. The differences between amplitudes were relatively low, especially for the inertial component. The most apparent mean differences were contributed by several occurrences of the situation, when in calibrated or impaired data a peak was found fulfilling the criteria stated in

Please cite this article in press as: O. Šprdlík, et al., Tremor analysis by decomposition of acceleration into gravity and inertial acceleration using inertial measurement unit, Biomed. Signal Process. Control (2010), doi:10.1016/j.bspc.2010.09.004

Table 1
Influence of calibration accuracy.

	Correlation		Mean difference (%)	
	Bias in a	Bias in ω	Bias in a	Bias in ω
A_{aiL}	0.99999999	0.999991	0.08	0.2
A_{aiG}	0.99999999	0.999998	0.08	0.2
A_{agL}	0.99998	0.9999	2.8	5.6

Sec. 2.4 and in the other not. The relative difference was 100% in such situation. Note that amplitudes A_{agL} were much lower than amplitudes of the inertial component (see Fig. 6 and Table 4).

Left: Pearson's correlation coefficients between amplitudes of 3D signals calculated from the calibrated sensors data and amplitudes calculated from the data corrupted by additional errors in acceleration (a) and angular rate (ω). The amplitudes were calculated from peaks in PSD of the signals.

Right: Mean relative differences between the original amplitudes and amplitudes from corrupted signals. Mean relative difference was defined as the mean of absolute values of the differences between the two values divided by the maxima of the two values, e.g. for the amplitude of inertial component A_{aiL} obtained from one measurement with the use of the calibrated data and the amplitude obtained with the acceleration corrupted by additional bias ($A_{aiL,\,\text{corrupted}\,a}$) the relative difference was $|A_{aiL} - A_{aiL,\,\text{corrupted}\,a}|/\max(A_{aiL},\ A_{aiL\,\text{corrupted}\,a})$. Where both amplitudes were zero, the relative difference was also considered zero.

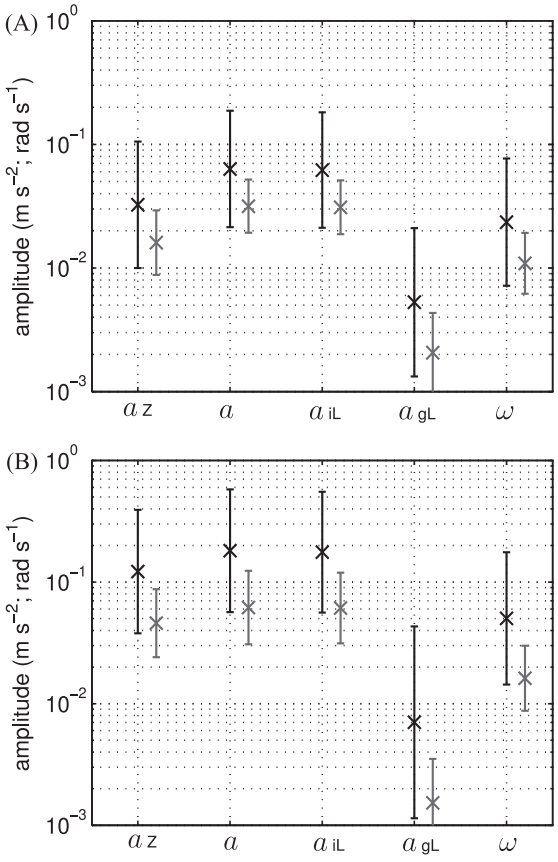

Fig. 6. Means and standard deviations of the amplitudes obtained from peaks in spectra of the measured acceleration in axis perpendicular to the hand a_Z, measured 3D acceleration a, movement acceleration in local coordinates a_{iL}, projection of gravity a_{gL}, and measured angular velocity ω. (A) Amplitudes from the test for rest tremor. (B) Amplitudes from all the tests for postural tremor. Means and standard deviations were computed in logarithmic coordinates. Left (black) bars correspond to the group of patients; right (gray) bars correspond to the group of healthy subjects.

Table 2
Correlation coefficients between amplitudes derived from spectral peaks of different signals.

	Corr. of amplitudes			Corr. of logarithms		
	A_{aiL}	A_{agL}	A_ω	A_{aiL}	A_{agL}	A_ω
A_a	0.999	0.92	0.93	0.9995	0.94	0.95
A_{aiL}		0.90	0.91		0.94	0.95
A_{agL}			0.996			0.97

Left: Correlations of amplitudes. Right: Correlations of amplitude logarithms. Correlations of A_{aiG} and its logarithms (not included in the table) with A_{aiL} and its logarithms were greater than 0.9998. Differences between their correlations with other quantities were lower than 0.0005.

Table 3
Correlation coefficients between tremor frequencies derived from different signals.

	Correlations of frequencies		
	f_{aiL}	f_{agL}	f_ω
f_a	0.96	0.71	0.68
f_{aiL}		0.67	0.65
f_{agL}			0.79

Differences between correlations of f_{aiG} (not included in the table) and f_{aiL} with others were lower than 0.0005.

3.2. Relationships between amplitudes and frequencies detected for different signals

The amplitudes and frequencies were compared in terms of correlation coefficients according to section 2.5. The cases where no peaks were detected in some of the signals were removed from this analysis. A peak was detected in PSD of a in 891 from 928 tests, in 895 cases for a_{iL}, 894 for a_{iG}, in 455 for a_{gL}, and in 878 for ω. Totally, 449 tests remained with peaks detected in all the signals.

Correlation coefficient for both raw amplitudes and their logarithms to base 10 are listed in Table 2. The most correlated amplitudes were A_{aiL} and A_{aiG}. They also correlate well with the amplitude of the measured acceleration (A_a). Amplitude of the gravitational component (A_{agL}) correlate better with the amplitude of angular rate (A_ω) than do these two amplitudes with amplitudes of other accelerations (A_a, A_{aiL}, A_{aiG}). The same holds for the logarithms of amplitudes.

Correlation coefficients between peak frequencies of different signals are listed in Table 3. The highest correlations are again for A_a, A_{aiL}, and A_{aiG} mutually. Frequency of a_{gL} correlates the most with the frequency of ω.

The amplitudes of the gravitational component of acceleration were lower than the amplitudes of inertial acceleration (about one-tenth, see Fig. 6 and Table 4).

Usually, the frequency of the detected peak was (at least approximately) the same from all signals where a peak was detected in the same test. In some cases the frequency differed notably (e.g. f_a and f_{agL}). In 238 tests from 928 the maximum difference between detected peaks was greater than 1 Hz. Most of these cases occurred in tests with signals of relatively low amplitudes. Part of the cases

Table 4
Ratios of amplitudes of gravitational and inertial acceleration.

	X	Y	Z	All
				Postural
Max	0.50	0.42	0.09	0.17
Average	0.18	0.11	0.02	0.07
Min	0.05	0.02	0.001	0.03
Rest				
Max	0.56	1.11	0.51	0.49
Average	0.09	0.14	0.10	0.12
Min	0.02	0.03	0.02	0.04

Please cite this article in press as: O. Šprdlík, et al., Tremor analysis by decomposition of acceleration into gravity and inertial acceleration using inertial measurement unit, Biomed. Signal Process. Control (2010), doi:10.1016/j.bspc.2010.09.004

involved such peaks that the frequency of one of them was approximately double of the frequency of another one. That may stem from the nonlinear properties of periodic movement with rotational character mentioned in the introduction.

3.3. Analysis in individual axes

More detailed analysis was done for the test on postural tremor with hands extended horizontally and for the test on rest tremor with hands hanging freely down from arm support. Amplitudes were computed not only from composite PSD of 3-component signals but also for all signal components separately. Hand axes were used instead of sensor axes. Ratios between amplitudes of gravitational artifact and inertial acceleration were studied

See Table 4 for ratios of gravitational and inertial acceleration amplitudes. In the test on postural tremor the ratio is notably lowest in the Z axis. That agrees with the results of the analysis realized in [4]. In the test on the rest tremor the difference between the mean ratios in individual axes is not so high – Z axis is more inclined from the vertical due to the hanging position of the hand and its sensitivity to changes of the gravitational component due to rotations is greater.

Mean and extremal ratios found between the amplitudes of gravitational artifact and inertial acceleration (A_{agL}/A_{aiL}) in tests for postural and rest tremor. The ratio is listed for different sensor axes as well as for the overall amplitudes of three-component signals. Cases where some of the two amplitudes was zero were not included in the averaging.

3.4. Differences between groups

Means and standard deviations of limited amplitude logarithms were computed. For the visualization they were transformed back to absolute values and shown in Fig. 6 in logarithmic coordinates.

In all signals both groups were far from having same mean amplitude logarithm ($P < 10^{-8}$). Not surprisingly, in tests for postural tremor the groups were distinguished better (see Fig. 6). The tests are known to be more suitable to distinguish the groups as postural tremor is more typical in essential tremor patients than rest tremor. The parameters of ROC curves were also extracted for amplitudes of each signal in all the tests for postural tremor taken together.

See Table 5 for the results. In most of separability measures, amplitudes of inertial acceleration (A_{aiL} and A_{aiG}) and the amplitude of measured acceleration (A_a) distinguished the groups best. The exception is the P-value in the first scenario that is lower for the amplitude of angular rate (A_ω). ROC parameters of A_ω are comparable to the parameters of A_a, A_{aiL}, and A_{aiG} in the first scenario.

In some parameters (P-value in both scenarios and potential classification accuracy in the first scenario), amplitudes of inertial components performed a little better than the amplitude of the measured acceleration. The amplitude derived from the acceleration measured in the approximately vertical axis (A_{aZ}) performed worse in all the parameters than A_a, A_{aiL}, and A_{aiG} and in most of the parameters worse than A_ω.

3.5. Regression of the visual assessment

The visual assessment of tremor severity by clinicians was interpolated by polynomials of different degrees and in different number of variables. Limited logarithms of amplitudes were used as the variables. See Section 2.8 for more details and Fig. 7 for an example. The proficiency of different regression function structures was quantified by root mean square error (RMSE) and by the percentage of predicted tremor scores that differed from the values assessed by clinicians by less than 1 with the use of the leave-one-out methodology. See Table 6 for an excerpt of results. For the sake of brevity, only several combinations of 2 and 3 amplitudes are shown, that reached the best RMSE. Only results for the two best polynomial degrees are presented for each amplitude combination shown, plus the results of the first degree polynomials with one variable (linear regression).

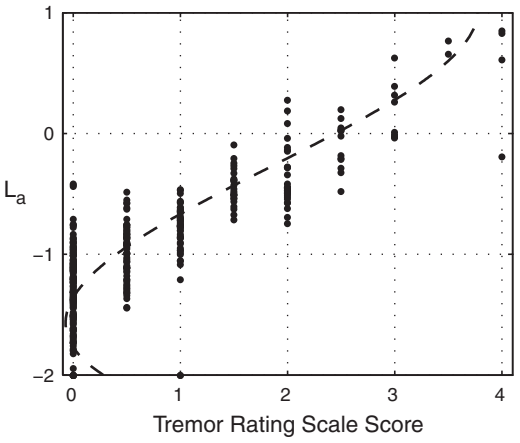

Fig. 7. Mean visual scores and corresponding limited logarithms of the amplitudes derived for the measured acceleration (L_a). Scores were regressed by a polynomial in L_a, degree = 3, dashed line.

From the first degree polynomials, the regression function using the angular rate amplitude had the lowest RMSE. However, when using the optimal degree, regression functions using amplitudes derived from measured and inertial acceleration performed better.

Using more than one amplitude in the regression function usually improved the proficiency. All the presented regression functions using two and three amplitudes performed better in RMSE than any regression function using only one amplitude. All the regression functions using two variables presented in the Table 6 also performed better or equally in the $\%_{E<1}$ parameter.

The optimal regression function structure, according to RMSE in the leave-one-out setting, was a polynomial of total degree 5 in logarithms of the three amplitudes derived from the angular rate, the inertial acceleration in the inertial frame and the inertial acceleration in the sensor frame. The error was 0.377 on the tremor rating scale.

For most amplitude combinations presented, the proportion of predictions with error lower than 1 was about 98%. The exceptions are 1D regression functions using A_{agL} and A_ω.

The proficiency of regression functions was presented for the polynomial degrees that were the best according to the root mean square error (RMSE) with the leave-one-out method used. The limited logarithms of the amplitudes listed were the variables of the polynomials. For the 2D and 3D polynomials, the numbers in the Degree columns correspond to degrees in the amplitude logarithms in the order as listed. Columns $\%_{E<1}$ contain the percentage of predicted tremor scores that differed from the values assessed by clinicians by less than 1. For the combinations of amplitudes listed in round brackets, $\%_{E<1}$ was the same as listed in the table, RMSE differed by less than 0.002. The choice of the polynomial degree that was the second best according to RMSE is presented for each combination of amplitudes listed in the table. The proficiency of linear regression functions (polynomial degree = 1) with one variable is presented too.

Coefficients of determination (r^2) and mean absolute errors (MAE) were also computed in the leave-one-out setting for the regression function structures presented in Table 6. From the linear functions, the one using A_ω was the best according to both criteria: $r^2 = 0.72$, MAE = 0.375. From the other regression functions, the

Please cite this article in press as: O. Šprdlík, et al., Tremor analysis by decomposition of acceleration into gravity and inertial acceleration using inertial measurement unit, Biomed. Signal Process. Control (2010), doi:10.1016/j.bspc.2010.09.004

Table 5
Measures of the separability of the groups of patients and controls in terms of tremor amplitude of postural tremor. Top: Tremor amplitude taken from a hand in one test. Bottom: Greater of the amplitudes from the left and right hand in one test. Best values (with some tolerance) are highlighted in bold.

	A_{aZ}	A_a	A_{aiL}	A_{aiG}	A_{agL}	A_ω
First scenario: A_α						
P-Value	2.1×10^{-35}	3.8×10^{-43}	2.2×10^{-43}	1.1×10^{-43}	3.7×10^{-40}	$\mathbf{1.3} \times 10^{-44}$
AUC	0.783	**0.809**	**0.808**	**0.809**	0.747	**0.808**
Potential accuracy (%)	74.4	**76.7**	**76.9**	**76.9**	73.6	76.1
Second scenario: max(A_α left, A_α right)						
P-Value	9.3×10^{-24}	7.2×10^{-26}	$\mathbf{1.5} \times 10^{-26}$	$\mathbf{1.5} \times 10^{-26}$	2.4×10^{-25}	1.5×10^{-25}
AUC	0.807	**0.834**	**0.833**	**0.833**	0.793	0.821
Potential accuracy (%)	78.7	**79.9**	**79.9**	**79.9**	77.9	77.3

P-value: *P*-values of two-sample *t*-tests applied to amplitudes of pNote that in the second scenario, the number of samples is half of the number in the first scenario. AUC: The area under the ROC curve. Potential accuracy: Percentage of correct group classifications with the amplitude thresholds set up optimally in terms of this criterion.

one using A_{aiL}, A_{aiG}, and A_ω, degree [1 2 2], was the best according to r^2 (0.83) and the one using A_{aiL} and A_ω, degree [5 2], was the best according to MAE (0.273). The coefficients of determination were greater than 0.8 and MAE lower than 0.3 for all the 2D and 3D regression function structures listed and for all the 1D polynomials of optimal degrees listed that use A_a or A_{aiL}.

4. Discussion

Findings about the ratio between the amplitudes of the estimates of the gravitational artifact and the inertial acceleration agree with the analytic findings about the component of gravitational artifact in [4]: The AC component of the gravitational artifact is relatively lowest in the (approximately) vertical axis and it is much greater in the other axes. The ratio implies that in other axes an error of up to tens of percent may occur if the measured acceleration is directly used to estimate the amplitude of spatial displacement by double integration.

Following the simplified model in [4], the ratio in the proximodistal hand axis in the first test for postural tremor should be notably higher than that in Table 4 and observed in the example in Fig. 3(c). The difference can be explained by differences between the measurement setup and the simplified model:

- The sensors were placed notably above the hand axis.
- Sensor/hand alignment and the orientation itself might be estimated inaccurately.
- Although the flexion–dorsiflexion movement of hands implying the high ratio in the model was typical in the used test for postural tremor, other movements also occurred.

Amplitudes and frequencies derived from the estimated 3D gravitational artifact correlate more with amplitudes and frequencies of the angular rate than do amplitudes and frequencies of the estimated inertial acceleration. That agrees with the fact that any changes in the gravitational component are only caused by rotations.

Several measures were used to quantify the performance of amplitudes of different signals to distinguish the group of patients from healthy subjects: parameters of the ROC curve and the two-sample *t*-test applied to amplitude logarithms. The amplitudes of the 3D measured and inertial acceleration (A_a, A_{aiL}, A_{aiG}) and the amplitude of angular rate (A_ω) distinguished the groups best according to different criteria. All these amplitudes performed better in most of the measures than the single accelerometer axis perpendicular to the hand that is used widely in the literature. In some separability measures, the amplitudes of the inertial component performed better than the amplitude of the measured acceleration. However, the differences were low.

Polynomial regression functions with suitable inputs and polynomial degrees were able to predict the visual assessment of tremor intensity with the root mean square error under 0.4. In about 98% of the measurements they predicted the score with the error lower than 1. The performance was very good with respect to the fact that the resolution of the visual assessment was 1 (0.5 when averaging two raters with different rates). The regression functions using several amplitudes including the amplitude of inertial component performed a little better than if using the measured acceleration instead of the inertial component.

A number of other works deal with the regression or correlation of a visual rating with quantities from an instrumented assessment. Part of them deal with a long-term ambulatory monitoring of tremor [13,22,23], other part use short measurements in defined hand positions [14,15,24,25]. The first approach differs from this study as the data were captured and averaged in long time intervals on one hand, but the setup was more relaxed on the other hand – even measurements from free movement of persons were included. In the second approach, the setup was tighter than our: The regression was done for a particular task and well defined hand position each time. Moreover, various clinical scales were used in the studies as the quantities to regress (or to use as regressors of measured amplitudes). Due to these facts, it cannot be judged which regression was of the best quality directly by comparing the coefficients of determination, residual errors, etc.

Table 6
Results of the regression of the visual assessment.

Amplitudes used	Degree (best)	RMSE	$\%_{E<1}$	Degree (2nd best)	RMSE	$\%_{E<1}$	RMSE (degree = 1)	$\%_{E<1}$
A_a	7	0.402	98.0	8	0.403	98.0	0.502	96.9
A_{aiL} (A_{aiG})	7	0.403	98.0	8	0.404	98.0	0.498	96.9
A_{agL}	7	0.516	94.1	5	0.517	93.5	0.655	89.5
A_ω	5	0.453	95.5	7	0.454	95.5	0.481	95.5
A_{aiL}, A_ω (A_{aiG}, A_ω)	10 1	0.380	98.0	5 2	0.381	98.0		
A_a, A_ω	5 2	0.384	98.0	6 2	0.384	98.0		
A_{aiL}, A_{agL} (A_{aiG}, A_{agL})	3 2	0.389	98.3	2 3	0.391	98.3		
A_{aiL}, A_{aiG}, A_ω	1 2 2	0.377	98.0	2 1 2	0.378	98.0		
A_{aiL}, A_{agL}, A_ω (A_{aiG}, A_{agL}, A_ω)	3 1 1	0.384	97.7	1 3 1	0.394	98.0		
A_{aiL}, A_{aiG}, A_{agL}	1 1 3	0.387	98.3	2 1 2	0.387	98.0		
A_a, A_{agL}, A_ω	3 1 1	0.387	97.5	1 3 1	0.396	98.0		

Please cite this article in press as: O. Šprdlík, et al., Tremor analysis by decomposition of acceleration into gravity and inertial acceleration using inertial measurement unit, Biomed. Signal Process. Control (2010), doi:10.1016/j.bspc.2010.09.004

A specialized time-domain algorithm using data from accelerometers placed on forearms was presented in [21] to assess in daily life the tremor amplitude and the proportion of time with tremor present. Other movements were also quantified beside tremor. The algorithm was further refined, ported to different hardware, and validated in [22,23]. Relatively long-term measurement and simultaneous minute-by-minute UPDRS rating of tremor amplitude were done. Tremor detection accuracy was good. High correlations were found between the obtained quantities and UPDRS when averaging over long time periods. The correlation of the estimated mean tremor duration with the mean clinical score was as high as $r = 0.96$ (r^2 about 0.92) in [22]. However, without averaging, the correlations of minute-by-minute quantities were published only within subjects, causing them relatively low due to a limited variation of tremor amplitude and occurrence in a single subject: Mean correlation coefficient was 0.71 (corresponding to r^2 about 0.5) in [22].

In [13] another method was proposed to quantify tremor in daily life using gyroscopes placed on forearms instead of accelerometers. The algorithm was tested on a sample of 10 patients with Parkinson's disease (PD) and 10 control subjects. Very high sensitivity and specificity was found when detecting tremor in periods of 3 seconds in a long protocol when compared to the visual assessment from a video recording. Correlations up to $r = 0.87$ (r^2 about 0.76) were found between an UPDRS tremor subscore (items 20 + 21, rest and action tremor) and mean logarithm of amplitudes computed from measurement in a 45 min long fixed protocol. The protocol was performed immediately after the UPDRS rating. Similar correlation was found in a free-move setting when averaging amplitude logarithms in periods of 30 or 45 min preceding the UPDRS evaluations.

A wide range of clinical scales and instrumented assessments at several institutions was studied in [24]. Two regressions respecting approximately logarithmic relations of amplitudes and clinical scores were done, one of them being linear regression with the use of the amplitude logarithm as the independent variable. The instrumented assessment was based on short-time measurements, but the visual assessment was not done simultaneously. In some sub-studies, the assessment was done immediately before or after the measurement. In others, the time lag was up to several weeks. In one sub-study, scores assessing social handicap and amount of water spilled when pouring from one tube to another were used instead of a direct visual assessment of the tremor amplitude. Coefficients of determination were computed from the published correlation coefficients. The coefficients range from $r^2 = 0.17$ (for a 0–3 scale, spilled water) and 0.30 (for a 0–4 scale, visual amplitude) to 0.74 in sub-studies using accelerometers, from $r^2 = 0.65$ to 0.78 in sub-studies using digitizing tablets, and $r^2 = 0.89$ in a sub-study using the linkage device [15]. The latter result is very good. However, each regression function was trained to a particular arm position and the correlations were computed for all the data available, no leave-one-out or similar methodology was used in [15,24]. Instead, standard errors of the estimated slopes of regression lines were estimated, being about 10% of the values, see [24], Table 2. On the other hand, all their results may suffer from the fact that the acquisition of the amplitude and the visual rating by a clinician were not synchronized.

In [14], visual score of the postural and rest tremor in PD patients was regressed using short-time accelerometer and gyroscope measurements. Measurements were done simultaneously with video recordings used for the visual assessment. The regression results for the rest/postural tremor were $r^2 = 0.89/0.90$ when using all the data, and $r^2 = 0.85/0.88$, RMSE = 0.32/0.35 when using the leave-one-out approach. The performance measures are better than ours. However, the resolution of the visual scale they used was more fine than the scale we used (see [14], Fig. 6), reducing the error caused by the discrete nature of clinical scales. Moreover, the regression function was trained to assess a concrete type of tremor in a concrete hand posture while we included several hand postures. In [14], all amplitudes from separate sensor axes were used while we used only the overall amplitudes derived from the composite spectra of 3D signals. On the other hand, only linear functions of the amplitude logarithms were used as regression functions in [14], while we used more general polynomials besides the linear regression by one amplitude logarithm.

Paper [25] extends [14] by correlations with another visual scale used to quantify the postural and kinetic tremor in patients with the essential tremor. A relatively small sample of tremor assessments was used in the study. The correlation between the score provided by the used system and the visual score in the postural tremor was $r = 0.738$ (r^2 about 0.54) and error MAE = 0.42. The found accuracy of the regression is lower than our results. The accuracy may suffer from the fact that they used much smaller sample of data from a similar number of subjects as we involved.

5. Conclusions

Estimates of the inertial acceleration caused purely by a translational movement in the inertial frame and of the gravitational artifact were used for tremor quantification in addition to the actually measured acceleration and angular rate. The decomposition of the acceleration into the two components was performed with the use of an orientation (posture, pose, attitude) estimation using the data provided by the inertial measurement unit.

The orientation estimation accuracy was not directly validated using any alternative methodology, but low sensitivity of the proposed detection scheme to corruption of the measured data with constant bias was demonstrated. It appears that high accelerations of a severe tremor may influence the orientation estimate. An analysis of this influence and its reduction may be a subject of future investigations.

The performance in separating the group of patients from healthy persons and in the regression of the visual tremor rating was good and comparable to the results presented in other publications. 3D accelerometry was more efficient in separating the groups than uniaxial accelerometry. The use of the decomposed acceleration further improved the performance in both tasks. However, the differences were low and further investigation may be needed to make a definite conclusion about the better suitability of the acceleration components for tremor detection and quantification when compared to raw measured signals.

Other movement variables like position or linear velocity are often used as the quantities for tremor analysis as they are better related to visual observations by a human. In the future work, they may be estimated from the acceleration and investigated beside the variables from the presented work in order to find reasonable representation of tremor intensity and frequency without dependence on particular hand position. More information about the movement may be also extracted and utilized for the regression or classification if quantifying amplitudes in separate axes instead of the single amplitude for a 3D signal. In such a case, separating the gravitational component may be more helpful, as the amplitude of its spectral peak manifests more in some particular axes than in the case when the amplitudes derived from 3D acceleration are used.

Acknowledgment

The authors wish to thank Zdenka Uhríková, MSc. and Marie Kofránková, MD for their kind assistance. Filter for estimation of orientation was implemented using ReBEL: Recursive Bayesian Estimation Library for Matlab obtained from OGI School of Science and Engineering, Rudolph van der Merwe and Eric A. Wan

under academic license. This work was supported by grants from the Czech Ministry of Education, 1M0567 and VZ MSM0021620849, and Czech Ministry of Health, IGA NR9215.

References

[1] G. Deuschl, P. Bain, M. Brin, Ad hoc scientific committee, consensus statement of the Movement Disorder Society on tremor, Mov. Disord. 13:S3 (1998) 2–23.
[2] E.D. Louis, S.L. Pullman, Comparison of clinical vs. electrophysiological methods of diagnosing of essential tremor, Mov. Disord. 16 (2001) 668–673.
[3] R.J. Elble, Characteristics of physiologic tremor in young and elderly adults, Clin. Neurophysiol. 114 (2003) 624–635.
[4] R.J. Elble, Gravitational artifact in accelerometric measurements of tremor, Clin. Neurophysiol. 116 (2005) 1638–1643.
[5] F. Foerster, M. Smeja, Joint amplitude and frequency analysis of tremor activity, Electromyogr. Clin. Neurophysiol. 39 (1999) 11–19.
[6] S. Morrison, J. Kavanagh, S.J. Obst, J. Irwin, L.J. Haseler, The effects of unilateral muscle fatigue on bilateral physiological tremor, Exp. Brain Res. 167 (2005) 609–621.
[7] P.H. Veltink, E.G. Olde Engbering, B.J. van Hilten, R. Dunnewold, C. Jacobi, Towards a new method for kinematic quantification of bradykinesia in patients with Parkinson's disease using triaxial accelerometry, in: IEEE 17th Annual Conf. Eng. in Medicine and Biology Soc., 1995, pp. 1303–1340.
[8] E.J.W. van Someren, R.H.C. Lazeron, B.F.M. Vonk, M. Mirmiran, D.F. Swaab, Gravitational artefact in frequency spectra of movement acceleration: implications for actigraphy in young and elderly subjects, J. Neurosci. Methods 65 (1996) 55–62.
[9] J.D. Frost jr., Triaxial vector accelerometry: a method for quantifying tremor and ataxia, IEEE Trans. Biomed. Eng. 25 (1978) 17–27.
[10] A.M. Kuncel, S.E. Cooper, B.R. Wolgamuth, W.M. Grill, Amplitude- and frequency-dependent changes in neuronal regularity parallel changes in tremor with thalamic deep brain stimulation, IEEE Trans. Neural Syst. Rehabil. Eng. 15 (2007) 190–197.
[11] P.R. Burkhard, J.W. Langston, J.W. Tetrud, Voluntarily simulated tremor in normal subjects, Neurophysiol. Clin. 32 (2002) 119–126.
[12] E. Rocon de Lima, A.O. Andrade, J.L. Pons, P. Kyberg, S.J. Nasuto, Empirical mode decomposition: a novel technique for the study of tremor time series, Med. Bio. Eng. Comput. 44 (2006) 569–582.
[13] A. Salarian, H. Russmann, C. Wider, P.R. Burkhard, F.J.G. Vingerhoets, K. Aminian, Quantification of tremor and bradykinesia in Parkinson's disease using a novel ambulatory monitoring system, IEEE Trans. Biomed. Eng. 54 (2007) 313–322.
[14] J.P. Giuffrida, D.E. Riley, B.N. Maddux, D.A. Heldman, Clinically deployable Kinesia technology for automated tremor assessment, Mov. Disord. 24 (2009) 723–730.
[15] J.Y. Matsumoto, D.W. Dodick, L.N. Stevens, R.C. Newman, P.E. Caskey, W. Fjerstad, Three-dimensional measurement of essential tremor, Mov. Disord. 14 (1999) 288–294.
[16] G. Deuschl, R. Wenzelburger, K. Löffler, J. Raethjen, H. Stolze, Essential tremor and cerebellar dysfunction: Clinical and kinematic analysis of intention tremor, Brain 123 (2000) 1568–1580.
[17] J.M. Spyers-Ashby, M.J. Stokes, P.G. Bain, S.J. Roberts, Classification of normal and pathological tremors using a multidimensional electromagnetic system, Med. Eng. Phys. 21 (1999) 713–723.
[18] W.T. Ang, P.K. Khosla, C.N. Riviere, Design of all-accelerometer inertial measurement unit for tremor sensing in hand-held microsurgical instrument, in: Proc. 2003 IEEE Int. Conf. Robotics and Automation, pp. 1781–1786.
[19] W.T. Latt, U.X. Tan, C.Y. Shee, C.N. Riviere, W.T. Ang, Compact sensing design of a handheld active tremor compensation instrument, IEEE Sens. J. 9 (2009) 1864–1871.
[20] R.A. Hyde, L.P. Ketteringham, S.A. Neild, R.J.S. Jones, Estimation of upper-limb orientation based on accelerometer and gyroscope measurements, IEEE Trans. Biomed. Eng. 55 (2008) 746–754.
[21] E.J.W. van Someren, W.A. van Gool, B.F.M. Vonk, M. Mirmiran, J.D. Speelman, D.A. Bosh, D.F. Swaab, Ambulatory monitoring of tremor and other movements before and after thalamotomy: a new quantitative technique, J. Neurol. Sci. 117 (1993) 16–23.
[22] E.J.W. van Someren, B.F.M. Vonk, W.A. Thijssen, J.D. Speelman, P.R. Schuurman, M. Mirmiran, D.F. Swaab, A new actigraph for long-term registration of the duration and intensity of tremor and movement, IEEE Trans. Biomed. Eng. 45 (1998) 386–395.
[23] E.J.W. van Someren, M.D. Pticek, J.D. Speelman, P.R. Schuurman, R. Esselink, D.F. Swaab, New actigraph for long-term tremor recording, Mov. Disord. 21 (2006) 1136–1143.
[24] R.J. Elble, S.L. Pullman, J.Y. Matsumoto, J. Raethjen, G. Deuschl, R. Tintner, and the Tremor Research Group, Tremor amplitude is logarithmically related to 4- and 5-point tremor rating scales, Brain 129 (2006) 2660–2666.
[25] G. Mostile, J.P. Giuffrida, O.R. Adam, A. Davidson, J. Jankovic, Correlation between kinesia system assessments and clinical tremor scores in patients with essential tremor, Mov. Disord. (2010), ahead of print.
[26] S. Fahn, E. Tolosa, C. Marín, Clinical rating scale for tremor, in: J. Jankovic, E. Tolosa (Eds.), Parkinson's Disease and Movement Disorders, second ed., Williams and Wilkins, Baltimore, 1993, pp. 271–280.
[27] J.C. Lötters, J. Schipper, P.H. Veltink, W. Olthuis, P. Bergveld, Procedure for in-use calibration of triaxial accelerometers in medical applications, Sens. Actuators A Phys. 68 (1998) 221–228.
[28] N. Grammalidis, M.G. Strintzis, Using 2-D and 3-D ellipsoid fitting for head and body segmentation and head tracking, in: International Conference on Image and Multidimensional Digital Signal Processing, 1998.
[29] S.J. Julier, J.K. Uhlmann, A new extension of the Kalman filter to nonlinear systems, in: Proc. Int. Symp. Aerospace/Defense Sensing, Simul. and Controls, 1997.
[30] E.A. Wan, R. van der Merwe, The unscented Kalman filter, in: S. Haykin (Ed.), Kalman Filtering and Neural Networks, John Wiley & Sons, Inc., 2001, pp. 221–280.
[31] R. van der Merwe, E.A. Wan, Sigma-point Kalman filters for integrated navigation, in: Proc. of the 60th Annual Meeting of the Institute of Navigation (ION), 2004.
[32] B. Stevens, F. Lewis, Aircraft Control and Simulation, second ed., John Wiley & Sons, Inc., 2003.
[33] I. Markovsky, B. De Moor, Linear dynamic filtering with noisy input and output, Automatica 41 (2005) 167–171.
[34] OGI School of Science & Engineering, ReBEL: Recursive Bayesian Estimation Library for Matlab. 2008. Web: http://choosh.csee.ogi.edu/rebel, 6 Dec 2009.
[35] J.M. Spyers-Ashby, P.G. Bain, S.J. Roberts, A comparison of fast Fourier transform (FFT) and autoregressive (AR) spectral estimation techniques for the analysis of tremor data, J. Neurosci. Methods 83 (1998) 35–43.
[36] J. Timmer, Quantitative analysis of tremor time series, Electroencephalogr. Clin. Neurophysiol. 101 (1996) 461–468.
[37] P.S. Slack, X. Ma, Tremor amplitude determination for use in clinical applications, Meas. Sci. Technol. 18 (2007) 3471–3478.

Please cite this article in press as: O. Šprdlík, et al., Tremor analysis by decomposition of acceleration into gravity and inertial acceleration using inertial measurement unit, Biomed. Signal Process. Control (2010), doi:10.1016/j.bspc.2010.09.004